

The role of final state correlation in double ionization of helium: a master equation approach

Sølve Selstø,¹ Tore Birkeland,² Simen Kvaal,¹ Raymond Nepstad,³ and Morten Førre³

¹Centre of Mathematics for Applications, University of Oslo, N-0316 Oslo, Norway

²Department of Mathematics, University of Bergen, N-5020 Bergen, Norway

³Department of Physics and Technology, University of Bergen, N-5020 Bergen, Norway

(Dated: September 13, 2010)

The process of nonsequential two-photon double ionization of helium is studied by two complementary numerical approaches. First, the time-dependent Schrödinger equation is solved and the final wave function is analyzed in terms of projection onto eigenstates of the uncorrelated Hamiltonian, i.e., with no electron-electron interaction included in the final states. Then, the double ionization probability is found by means of a recently developed approach in which the concept of absorbing boundaries has been generalized to apply to systems consisting of more than one particle. This generalization is achieved through the Lindblad equation. A model of reduced dimensionality, which describes the process at a qualitative level, has been used. The agreement between the methods provides a strong indication that procedures using projections onto uncorrelated continuum states are adequate when extracting total cross sections for the direct double ionization process.

PACS numbers: 32.80.Fb, 32.80.Rm, 31.15.-p, 02.70.-c

I. INTRODUCTION

The problem of multiphoton single- and multiple ionization of atoms and molecules has been subject of intense research in recent years. The development of new high-frequency light sources, such as free-electron lasers (FEL) and high-order harmonic generation sources, capable of generating intense coherent radiation, is one reason for this. Pulses of attosecond durations are now routinely produced by high-order harmonic generation with intensities as high as 10^{14} W/cm² [1], enabling experimental studies of nonlinear phenomena in the extreme-ultraviolet regime in atoms [2, 3] and molecules [4]. Owing to recent advances in FEL technology, femtosecond pulses of unprecedentedly high intensity are now available, covering wavelengths ranging from vacuum ultraviolet to soft x-rays [5, 6]. These pulses have opened the door for experimental studies of multiphoton multiple ionization of complex atoms [7–9] and atom clusters [10]. A parallel development of *ab initio* numerical methods, capable of addressing the problem of intense-field multiphoton ionization in one- and two-electron systems has taken place [11–13].

Despite these developments, the problem of nonsequential (direct) two-photon double ionization of helium still remains an unsolved problem, even though it has been widely studied during the last decade both theoretically [14–28] and experimentally [3, 29–31]. The main obstacle in experiments has been to produce sufficiently high ionization yields. On the theoretical side, accurate predictions for the total (generalized) cross sections of the process remain elusive, as values obtained with different methods vary by more than an order of magnitude. What characterizes this particular two-photon process is that it depends upon exchange of energy between the outgoing electrons, i.e., it is a so-called nonsequential or direct process, as opposed to a sequential ionization process where both electrons may be considered as independent particles. The sequential process is energetically inaccessible for photon energies below 54.4 eV, but becomes the dominant two-photon ionization process at higher energies. Concerning the nonsequential process, the great discrepancies that remain

between different theoretical calculations are usually ascribed to the different ways electron correlations are handled. It has furthermore been claimed, by several authors, that the two-photon double ionization process in helium is a problem in which electron correlations in the final state play an extremely important role. This stands somewhat in contrast to the related (direct) one-photon double ionization process, where a complete agreement between different theoretical approaches and experiments is now established [19, 32–34].

As it turns out, it is especially the separation of the two-photon single ionization, where the remaining electron is left in an excited ionic state, from the two-photon double ionization that is the bottleneck, the main problem being that electrons are emitted with similar energies in the two processes. Moreover, the fact that the single ionization process is much more probable makes the problem even more challenging, and an exact knowledge of the role of correlation in the final state particularly important. The effect of electron correlations in the final state on the total integrated cross section was studied in detail by Fomouou *et al.* [19, 26]. Using the J-matrix method they were able to incorporate correlation effects in the final (single continuum) scattering states, with the result that their calculated generalized cross section increased significantly compared to the result they obtained when projecting the final wave packet directly onto uncorrelated products of Coulomb waves (with nuclear charge $Z = 2$) (compare full green curve with diamonds with full black curve with crosses in Fig. 1). More importantly, their uncorrelated result is in complete accordance with calculations performed by others [14, 16–18, 20, 24, 25, 28], which all have in common that the role of correlation was completely neglected in the final state. For comparison, these results, together with the result of Feist *et al.* [24] and Nepstad *et al.* [28], and available experimental data, is shown in Fig. 1.

Generating correlated multichannel states, and employing lowest-order (non-vanishing) perturbation theory, Nikolopoulos and Lambropoulos [23] obtained a value for the cross section that differed even more substantially from the uncorrelated results (black line with triangles in Fig. 1). From this

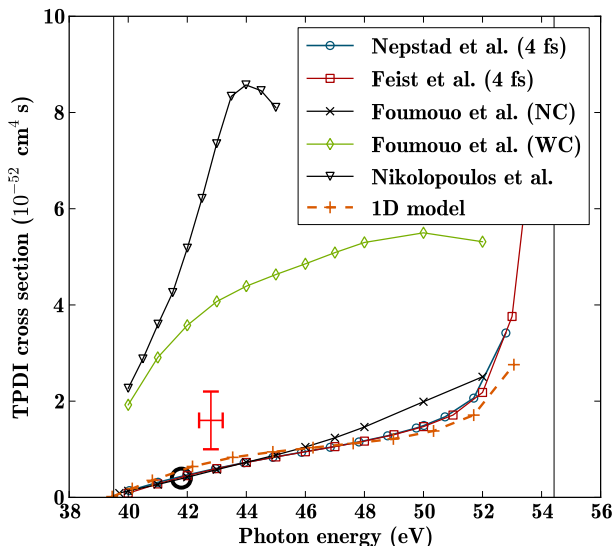


FIG. 1: (Color online) Two-photon double ionization cross sections. Black circle: experimental result of Hasegawa *et al.* [29], red cross: experimental result of Sorokin *et al.* [30], blue line with circles: the results obtained by Nepstad *et al.* [28], red line with squares: Feist *et al.* [24], green line with diamonds: Fomouuo *et al.* [19] (with correlation, WC), black line with crosses: Fomouuo *et al.* [19] (no correlation, NC), orange dashed line with '+' (scaled): 1D result with the Hamiltonian (1), and black line with triangles: Nikolopoulos *et al.* [23]. The vertical lines define the two-photon direct double ionization region.

observation, it appears reasonable to conclude that the inclusion of electron correlation in the final states is required. However, the R-matrix calculations by Feng and van der Hart [15], calculations employing exterior complex scaling by Horner *et al.* [22], and the time-dependent close-coupling calculations by Ivanov and Kheifets [21], which all consider final state correlations, produce results that are similar to the uncorrelated results. Thus, at present, the matter remains unresolved.

In this article, we revisit the problem of nonsequential two-photon double ionization of helium. We employ an approach based on the concept of absorbing boundaries and the Lindblad formalism [35] to calculate the generalized cross section for the process. Absorbing boundary conditions are often quite useful in the context of wave packet propagation [36–38]. However, applying them in the study of systems consisting of several particles is not straightforward. This is due to the fact that when one particle is absorbed, the Schrödinger equation does not retain any information about the remaining particles. Here we will demonstrate how the notion of absorbing boundary conditions may be generalized to apply to many-particle systems in such a way that single and double ionization may be distinguished [35]. Specifically, the method allows for describing the dynamics of the remaining electron as the first one is absorbed due to photoionization. A distinct advantage is that an exact knowledge of the final scattering states is superfluous. Furthermore, a direct comparison with the result obtained by projecting the final wave function onto

eigenstates of the uncorrelated Hamiltonian reveals that this procedure indeed is adequate, as a complete agreement between the two different methods is demonstrated.

Describing a helium atom exposed to a laser pulse numerically is a challenging task both in terms of algorithm and computational power. Several theoretical studies of this system involves models of reduced dimensionality [39–43]. Only during recent years has a full three-dimensional (3D) description become numerically feasible. The formalism based on the Lindblad equation involves resolving the dynamics of a one-particle density matrix in addition to a two-particle wave function – both involving six degrees of freedom when describing the full 3D problem. Since these two sub-systems are coupled, more involved numerical schemes are necessary when solving these equations than in the case of the time-dependent Schrödinger equation (TDSE). Thus, we resort to a one-dimensional (1D) model atom in the present work. We argue, however, that the coincidence between the double ionization probabilities obtained by the two different methods do shed light on the question of whether projection onto uncorrelated final states is an adequate approach also in the 3D case.

Having validated the Coulomb-wave projection method, we next consider the convergence property of the cross section in the vicinity of the threshold at 54.4 eV. It has been reported that the cross section exhibits an apparent divergence in this limit [20, 22, 24, 27, 44], a behavior that is usually interpreted as being due to an unwanted inclusion of the sequential process in the calculations caused by the bandwidth of the pulse [45, 46]. However, it has recently been shown that this rise cannot solely be attributed to such an effect [28]. That 3D study was limited to photon energies below 52 eV. Going beyond the 52 eV limit would require the application of extremely long pulses with durations of several tens of femtoseconds, which ultimately becomes an unmanageable problem in 3D. A 1D model remains computationally tractable, however, even for these long pulses, thus allowing to study the behavior of the cross section very close to the threshold.

In the following section the theory is outlined. Specifically, Sec. II A describes the model and discusses to what extent it is able to make predictions also valid for the full 3D system. The two different methods used in order to obtain total cross sections are described in Secs. II B and II C. Their implementation, and possible extension to 3D is discussed in Sec. II D. The comparison between the two methods is presented in Sec. III. Furthermore, the behaviour of the cross section when the photon energy approaches the threshold at 54.4 eV is discussed. Conclusions are drawn in Sec. IV.

II. THEORY

A. The model atom

The Hamiltonian of the system is given by

$$H = h(x_1) + h(x_2) + V_{\text{Int}}(x_1, x_2) \quad (1)$$

$$h(x) = -\frac{1}{2} \frac{d^2}{dx^2} + V_{\text{Nucl}}(x) + xE(t) \quad (2)$$

where x_i is the position of particle i and E is some external time-dependent electric field of finite duration T . Here, we have introduced atomic units, denoted ‘‘a.u.’’, which are defined by choosing the electron mass, the electron charge and \hbar as units for their respective quantities. Both the interaction with the nucleus, V_{Nucl} , and the electron-electron interaction, V_{Int} , are taken as regularized Coulomb potentials, instead of bare Coulomb potentials, i.e.,

$$V_{\text{Nucl}}(x) = -\frac{Z_{\text{Nucl}}}{\sqrt{x^2 + \delta^2}} \quad (3)$$

$$V_{\text{Int}}(x_1, x_2) = \frac{Z_{\text{Int}}}{\sqrt{(x_1 - x_2)^2 + \delta^2}}. \quad (4)$$

By choosing $Z_{\text{Nucl}} = 1.1225$, $Z_{\text{Int}} = 0.6317$ and $\delta = 0.3028$ a.u., the ground state and the first and second ionization thresholds coincide with those of the 3D case. We emphasize that it is crucial that also the second ionization threshold, i.e., the first excited state of He^+ , is correctly reproduced. For the photon energies considered here, it means that one-photon excitations of He^+ is not possible, concordant with the 3D case; indeed, such a possibility would introduce artifacts detrimental to our present purpose.

While these are necessary conditions for the model to produce results comparable with the original system, we cannot take for granted that they allow for conclusions pertinent to the real 3D to be drawn. Crucial geometrical aspects may potentially be lost when reducing the dimensionality of the problem. For instance, in the case of one-photon double ionization of helium, it is known that back-to-back scattering of the two electrons is prohibited for equal energy sharing [26]. Moreover, electron ejection is more probable in directions perpendicular to the polarization axis than parallel to it. Thus, for such a process, our 1D model cannot be expected to provide relevant information. For two-photon double ionization, however, it is known that back-to-back emission along the polarization axis is the dominating mode of ionization [26]. Such a process is indeed described within the 1D model.

Predictions for the angular aspects of the double ionization process, such as the directional distribution of the photoelectrons, cannot be made within the model. However, when it comes to the total cross section, it has been argued that for the process at hand, radial correlations, as opposed to angular correlations, provide the dominant contribution [47]. Hence, it seems reasonable to expect that the model should be able to describe the non-sequential double ionization process at a qualitative level. This assumption is strengthened by the fact that the 1D cross section, albeit too low in absolute value, does resemble the full 3D cross section as far as the photon energy is concerned, see Fig. 1.

In addressing the issue of whether projection onto uncorrelated final states provide the correct double ionization probability asymptotically, it is crucial not to underestimate the role of the electron-electron interaction. In the asymptotic region, both the nuclear potential and the electron-electron repulsion of the model coincide with the 3D case. Moreover, 1D models actually tend to *overestimate* correlation. This can be understood from the fact that the ‘‘smoothing’’ of the

Coulomb potential, Eq. (3), effectively reduces the kinetic energy of the system, which in turn increases the importance of correlation [48]. In our model, this is confirmed by comparing the expectation value of the kinetic energy T for the ground state with that of the original system; in 1D we find that $\langle T \rangle = 0.685$ a.u., which is about a fourth of the value found in 3D. The same tendency is found when comparing the correlation energy of the ground state; a Hartree-Fock calculation for the 1D model gives a ground state energy which is off by about 18 % as opposed to 1.4 % in the 3D case [49]. Thus, we expect electron-electron correlation to be at least as important in the 1D model as in 3D.

We note that, as the Hamiltonian is independent of electron spin, and the initial state is a spin eigenstate with symmetric spatial part, the system may be described formally as a two-boson system *without* spin. This will simplify the notation in the following.

B. Uncorrelated final state approach

In the method of projection onto uncorrelated final states, following Refs. [14, 16–18, 20, 24, 25, 28], we start out by diagonalizing the one-particle Hamiltonian h of Eq. (2), $h \phi_n = \varepsilon_n \phi_n$. The ‘‘uncorrelated double continuum’’ is defined by the span of two-particle symmetric states with positive energies,

$$\Phi_{m,n}^{\text{UCC}} = N_{m,n} [\phi_m(x_1) \phi_n(x_2) + \phi_n(x_1) \phi_m(x_2)] \quad (5)$$

$$\text{with } \varepsilon_m, \varepsilon_n > 0 \quad \text{and} \quad N_{m,n} = \begin{cases} \frac{1}{\sqrt{2}}, & m < n \\ \frac{1}{2}, & m = n \end{cases}.$$

Clearly, these states do not represent the actual double continuum states of the system. However, assuming that the electron correlation diminishes in significance as the doubly ionized wave packet travels outwards, the correct double ionization probability should be obtained by projecting the unbound part of the final state wave function at sufficiently long time after the interaction onto the uncorrelated continuum states,

$$P_{\text{DI}} = \sum_m \sum_{n \geq m} |\langle \Phi_{m,n}^{\text{UCC}} | \mathcal{P}_{\text{UB}} | \Psi(t \rightarrow \infty) \rangle|^2, \quad (6)$$

where the projection operator \mathcal{P}_{UB} removes the bound part.

C. Absorbing boundaries and the Lindblad equation

We seek to determine the validity of the above approach by comparing the double ionization yields thus obtained to the ones obtained using absorbing boundaries. These are introduced by augmenting the Hamiltonian with a complex absorbing potential, $-i\Gamma(x)$. The function $\Gamma(x)$ is zero within a certain region of x and beyond this region it is positive and increasing with distance,

$$\begin{aligned} \Gamma(x) &= 0, & |x| \leq x_T \\ \Gamma(x) &> 0, & |x| > x_T. \end{aligned} \quad (7)$$

Waves entering into the region where $\Gamma > 0$ are attenuated and eventually die out completely.

Simply introducing the absorber in the TDSE is problematic when we wish to distinguish between single and double ionization. This becomes evident when considering the fact that the wave function is normalized to the probability of *all* particles being represented. If one electron travels outwards and is subsequently absorbed, not only is all information about this electron lost, but so is all information about the remaining electrons as well. Thus, only information about total ionization probabilities may be retained when using an absorber in combination with the TDSE, while distinguishing between single, double etc. ionization is hard to achieve.

In a recent paper it was demonstrated how the notion of absorbing boundaries may be generalized to an N -particle context in such a way that the remaining $(N - 1)$ -particle system is recovered after one particle has been absorbed from the system [35]. Likewise, the $(N - 2)$ -particle system is recovered when yet another particle is absorbed etc. It was argued that, since this is a Markovian process, the Lindblad equation is the proper framework within which to achieve this [50, 51]. In general, the dynamics of a system where particles are lost due to a complex absorbing potential is described by [35]

$$i\hbar \frac{d}{dt} \rho_n = [\hat{H}, \rho_n] - i\{\hat{\Gamma}, \rho_n\} + 2i \int \Gamma(\xi) \psi(\xi) \rho_{n+1} \psi^\dagger(\xi) d\xi, \quad (8)$$

where ρ_n is the density operator corresponding to the n -particle sub-system, $n = 0, 1, \dots, N$. The generalized coordinates ξ correspond to *all* degrees of freedom. The operators $\psi(\xi)$ and $\psi^\dagger(\xi)$, which annihilate and create, respectively, a particle with position and spin given by ξ , obey the usual anti-commutation relations for fermions:

$$\{\psi(\xi), \psi(\xi')\} = 0, \quad \{\psi(\xi), \psi^\dagger(\xi')\} = \delta(\xi - \xi'). \quad (9)$$

The operators \hat{H} and $\hat{\Gamma}$ are the Hamiltonian and the complex absorbing potential, respectively, expressed in terms of these field operators such that their explicit forms do not depend on the particular number of particles. Specifically, for the two-particle system at hand the evolution may be written as

$$i\hbar \frac{d}{dt} |\Psi_2\rangle = (H - i\Gamma(x_1) - i\Gamma(x_2)) |\Psi_2\rangle \quad (10)$$

$$i\hbar \frac{d}{dt} \rho_1 = [h, \rho_1] - i\{\Gamma, \rho_1\} + \quad (11)$$

$$2i \int \Gamma(x) \chi(x) |\Psi_2\rangle \langle \Psi_2| \chi^\dagger(x) dx$$

$$\hbar \frac{d}{dt} \rho_0 = 2 \int \Gamma(x) \chi(x) \rho_1 \chi^\dagger(x) dx, \quad (12)$$

where $|\Psi_2\rangle$ is the two-particle state, ρ_1 is a one-particle density operator and $\rho_0 = p_0(t) |-\rangle \langle -|$ is a density operator corresponding to vacuum, i.e., no particles present. In Eqs. (10,11,12) the spin degree of freedom is integrated out. Hence the field operators $\chi^{(\dagger)}(x)$, which annihilate (create) a particle in position x , correspond formally to spinless bosons.

We emphasize that this formalism does not rely on the reduced dimensionality of the model. The equations remain the same regardless of the dimensionality of the coordinates x (or ξ).

We see that Ψ_2 follows the TDSE. Equation (11), which governs the evolution of the one-particle sub-system, has several terms. The first term on the right hand side, which corresponds to the von Neumann equation, simply governs the evolution of ρ_1 dictated by the one-particle Hamiltonian h . The second term corresponds to removal of the particle due to the absorber, whereas the last term is a source term depending on the overlap between the absorber and Ψ_2 . The decrease in norm of Ψ_2 is identical to the increase in the trace of ρ_1 induced by this source term, and the remaining electron is properly reconstructed. Similarly, the vacuum-probability p_0 increases by the same amount as $\text{Tr}(\rho_1)$ decreases due to absorption. These mechanisms are illustrated schematically in Fig. 2. The sum of all norms and traces remains equal to unity at all times [51], i.e.,

$$p_2(t) + p_1(t) + p_0(t) = 1, \quad \forall t \quad (13)$$

with $p_2(t) \equiv \|\Psi_2(t)\|^2$ and $p_1(t) \equiv \text{Tr}(\rho_1(t))$.

As also illustrated in Fig. 2, the density operator ρ_1 describes in general a mixed state,

$$\rho_1(t) = \sum_n p_1^{(n)} |\Psi_1^{(n)}(t)\rangle \langle \Psi_1^{(n)}(t)|, \quad (14)$$

i.e., one cannot in general expect a single-particle *wave function* since correlation information is lost whenever particles are removed.

In Fig. 3 we have shown $p_2(t)$, $p_1(t)$ and $p_0(t)$ as functions of time both during and after the interaction with the laser pulse. It is seen that the two-particle probability decreases during and after the pulse, whereas the one- and zero-particle probabilities increase – all towards some asymptotic value. It is also seen that $p_0(t)$ converges much more slowly than $p_2(t)$ and $p_1(t)$. We will return to this issue later. In the upper panel the probability for the system to remain in the ground state is also displayed. It shows that practically all population of bound states is confined to the ground state; very little excitation is seen.

The key point here is that as the first electron is absorbed, the dynamics of the remaining one may still be described. Moreover, if also the second electron is absorbed, we will eventually find the total system in the vacuum state. Now, suppose we may choose the absorption-free region large enough for the probabilities p_0 , p_1 and p_2 to converge towards values independent of x_T , then these probabilities are subject to straightforward interpretations: $p_2(t \rightarrow \infty)$ is the probability that the system remains bound after interaction, $p_1(t \rightarrow \infty)$ is the single ionization probability, and $p_0(t \rightarrow \infty)$ is the double ionization probability. This interpretation relies on the idea that there is a finite distance from the nucleus beyond which we may conclude that the electron is indeed in the continuum. The validity of this assumption, in turn, rests on whether the probabilities $p_1(t \rightarrow \infty)$ and $p_0(t \rightarrow \infty)$ converge as the absorber is moved outwards.

The ideal absorber should be both transmission and reflection free, and hence not influence the dynamics in the region

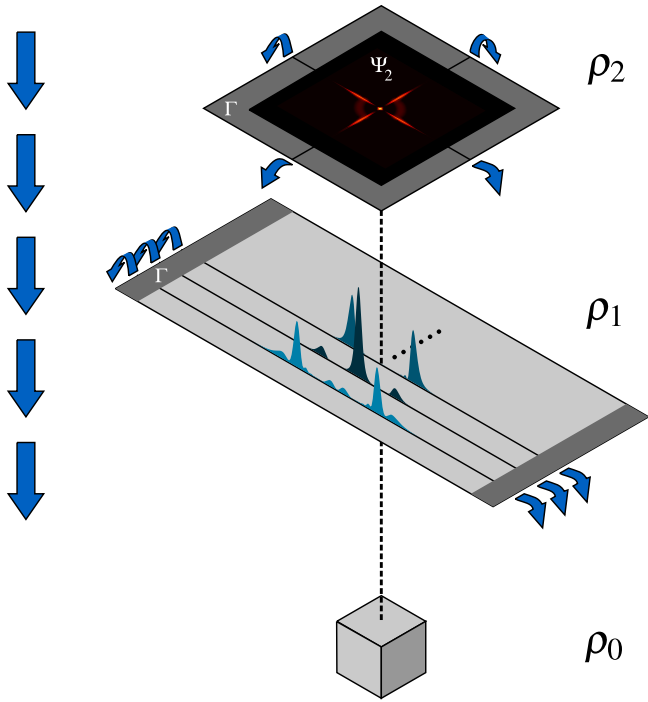


FIG. 2: (Color online) A schematic view of the absorbing boundary multi-particle method. The system is initially described by a two-particle wave function (top). As a particle is ionized and subsequently hits the absorber near the boundary (Γ), the remaining electron is described by a one-particle density matrix ρ_1 (middle level). Some of the eigenstates of ρ_1 are shown. Further ionization cause also ρ_1 to overlap with the absorber, which in turn causes the vacuum state to be populated. See text for further details.

where $\Gamma(x) = 0$ at all. In a many-body context, a certain indirect influence is difficult to avoid, however, since removal of one particle also removes the interaction between this particle and the remaining ones. This may be crucial if the field moves the electrons such that they are close while one of them is being absorbed. However, given a large enough x_T and long enough propagation time, the electron-electron repulsion itself should cause the importance of this interaction to diminish. Hence we conclude, once again, that the approach should be valid if one is able to obtain absorber-independent results.

As in the case of projection onto uncorrelated final states, the state of the system must be propagated a certain time beyond the duration T of the electric pulse in order for the double ionization probability p_0 to reach convergence. Having obtained the probability of direct double ionization, P_{DI} , for a situation in which perturbation theory applies, the total cross section for direct double ionization is found as [24, 52]

$$\sigma = \left(\frac{\omega}{I_0}\right)^2 \frac{P_{DI}}{T_{\text{eff}}}, \quad T_{\text{eff}} \equiv \int_0^T \left(\frac{I(t)}{I_0}\right)^2 dt, \quad (15)$$

where $I(t)$ is the intensity of the laser pulse, and I_0 is the maximum intensity. For a pulse with a sine square envelope,

$$E(t) = E_0 \sin^2\left(\frac{\pi t}{T}\right) \sin(\omega t + \varphi), \quad (16)$$

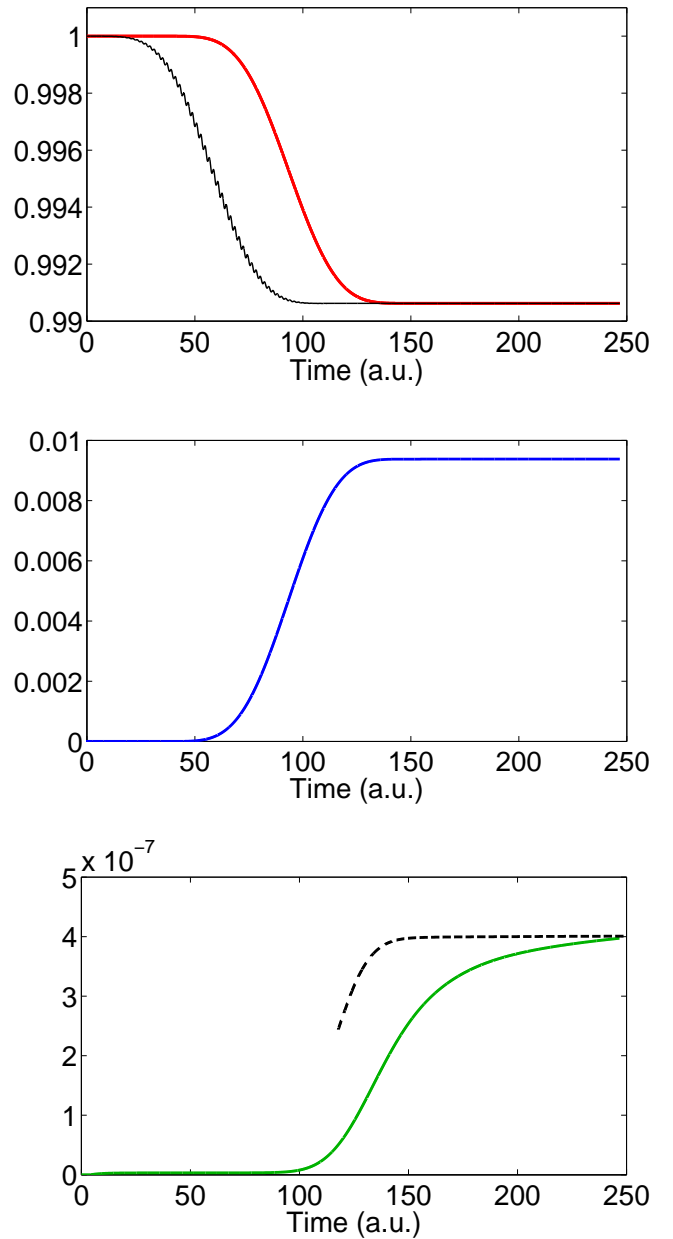


FIG. 3: (Color online) The probability of having two (upper panel), one (middle panel) or zero particles (lower panel) on the grid. The thin, black curve in the upper panel shows the probability for the system to remain in the ground state. The pulse duration is here $T = 118$ a.u. $= 2.86$ fs, the peak intensity is 2.2×10^{13} W/cm², and the central frequency of the pulse corresponds to a photon energy of 43.5 eV. We see that both the one-electron probability, $p_1(t) = \text{Tr}(\rho_1(t))$, and the zero-particle probability $p_0(t)$ increase as the norm of the two-particle probability, $p_2(t) = \|\Psi_2(t)\|^2$, decreases. The dashed curve in the lower panel represents the double ionization probability obtained by analyzing the absorbed part of the wave function “on the fly”. See text for details.

we have $T_{\text{eff}} = 35T/128$.

D. Numerical considerations

As mentioned in the introduction, one of the reasons for choosing a 1D model atom rather than trying to solve the full 3D problem is related to the implementation of Eqs. (10,11,12). While there are no *formal* obstacles prohibiting the application of the method to a 3D situation, and in spite of the fact that a grid of relatively small extension may be used, such calculations would generally involve very large basis sets. Thus, in a practical situation a parallelized version of the scheme is required. Since the two-particle dynamics is simply dictated by the Schrödinger equation, this part may be handled by any of a number of proposed parallel numerical schemes available in the literature [24, 28, 53], given the availability of sufficient computational resources. A similar scheme could then be adapted for the one-particle density matrix, Eq. (11). The remaining bottleneck is the calculation of the source term, which must be updated at each time step. Every part of the two-particle wavefunction at the previous time step which has a finite overlap with the absorber will contribute to the source term. This operation is potentially quite demanding on communication between the processing elements (PE), and some scheme to partially assemble the source term with the local data on each node is probably required, before these sub-elements may be transmitted to the correct PE for final assembly. Alternatively, the complexity of solving Eq. (11) could be reduced by a lower rank approximation, e.g., along the lines proposed by Leth and coworkers [54]. In any case, a non-parallel 1D model implementation is a natural starting point for further developments of the method, producing benchmarks and providing a convenient testing ground for determining optimal implementations of the various parts of the algorithm.

Returning to our 1D model, both the TDSE and Eqs. (10,11,12) are solved by means of split operator techniques [55] on uniform numerical grids, $x_i^j = -L/2 + (j-1)\Delta x$, where $i = 1, 2$ is the particle index, and $\Delta x = L/(\mathcal{N}-1)$, where \mathcal{N} is the number of grid points. The code solving the TDSE, implemented in the Pyprop framework [28, 56], is parallelized and thus able to handle relatively large grids.

The numerical scheme applied in order to solve Eqs. (10,11,12) was presented in [35]. However, here we have made some adjustments to the method in order to accommodate for two challenges which are both related to the long-range nature of the Coulomb interaction with the nucleus. Firstly, the system features Rydberg states, which may have a finite overlap with the absorber. If these states are populated, it could induce artificial ionization on large time scales. Hence, at $t = T$ all components of the bound states of the helium system was removed. These states, including the initial ground state, were found by propagation in imaginary time. Secondly, it is well known that photoelectrons of low kinetic energy may emerge from the process at hand [26]. This may be somewhat problematic since, as we have seen in Fig. 3, it causes $p_0(t)$ to converge rather slowly in time (it

takes the second electron a long time to reach the absorber). Moreover, the low energy of the photoelectron makes it vulnerable to artificial reflections induced by the absorbing potential. After the interaction with the laser pulse, $t > T$, this problem may be circumvented by analyzing the source term in Eq. (11) “on the fly” instead of propagating ρ_1 further. Suppose that the “amount” of double ionization is known at a time $t > T$, then at the next time step, $t + \Delta t$, the source term in Eq. (11) adds a contribution $(\Delta\rho_1)_S$ to the one-particle density operator. Since it is not very costly to diagonalize the one-particle Hamiltonian h , as compared to diagonalizing the full two-particle Hamiltonian H , this contribution $(\Delta\rho_1)_S$ may be separated into a part corresponding to bound He^+ and a (double) continuum part. The double ionization probability is then obtained simply by repeatedly adding (integrating) the latter contribution to the double ionization probability. Consequently, it is not necessary to solve Eqs. (11,12) for $t > T$ – as long as the absorbed part of Ψ_2 is properly analyzed. In the lower panel of Fig. 3 it is clearly demonstrated that the converged value for the double ionization probability is more easily obtained this way.

Note that during the interaction with the laser pulse, $t < T$, it is necessary to resolve the one- and zero-particle dynamics as well, since the remaining electron is still subjected to the electric field. We would like to point out that the formalism based on the Lindblad equation allows for analysis of the ionization channel yields using a grid that is smaller than the actual extension of the *complete* ionized wave packet. This holds also during interaction with the laser pulse.

For the Lindblad-formalism, practically convergent results for the double ionization probabilities were obtained using a box of size $L = 130$ a.u., a grid spacing of $\Delta x = 0.254$ a.u. and a numerical time step $\Delta t = 2.50 \times 10^{-3}$ a.u. For the complex absorbing potential we have chosen a Manolopoulos form, c.f. [57], which has several advantages such as being completely transmission free and only containing one parameter. We have fixed this parameter by the choosing $x_T = 0.2L$, c.f. Eq. (7). Finally we note that, due to trace conservation, Eq. (13), it is not strictly necessary to solve Eq. (12) along with Eqs. (10,11). However, since our numerical scheme is not manifestly unitary, we have still done so in order to check that Eq. (13) indeed is fulfilled to a satisfactory degree.

In the TDSE calculations, where the final wave packet is projected directly onto uncorrelated products of Coulomb waves (with nuclear charge $Z = 2$), Eq. (6), much larger boxes are required in order to contain the entire ionized wavepacket during the time evolution. We used $L \leq 2400$ a.u., which was sufficient for pulse durations up to 20 fs, and photon energies up to 53 eV. The grid resolution was fixed at $\Delta x = 0.195$ a.u., while the time step was $\Delta t = 5.00 \times 10^{-3}$ a.u.

III. RESULTS AND DISCUSSION

Figure 4 shows the total cross section for the process of nonsequential double ionization by two photons. Results have been obtained using both methods discussed above. In both cases, the electric field was given by Eq. (16). For lower

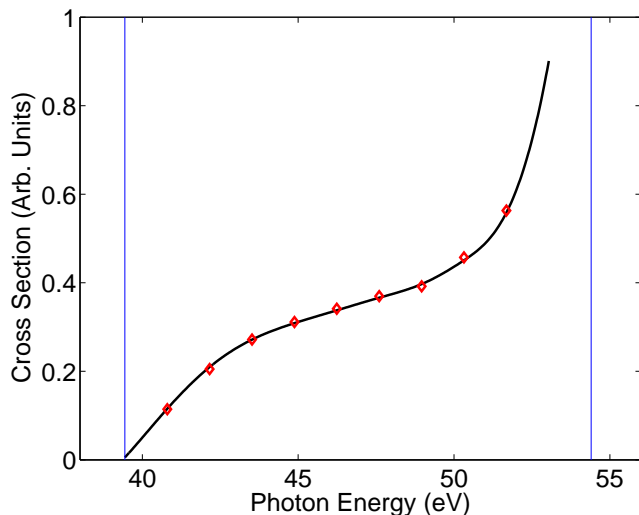


FIG. 4: (Color online) The (generalized) cross section for non-sequential two-photon double ionization of our 1D model helium atom. The full curve is obtained by solving the TDSE on a large grid with subsequent projection of the final wave packet directly onto uncorrelated products of Coulomb waves (with nuclear charge $Z = 2$). The diamonds are calculated by the method involving absorbing boundaries and the Lindblad equation.

photon energies the duration of the field corresponded to 30 optical cycles, whereas increasingly longer pulses were necessary in order to obtain converged cross sections as the photon energy increases towards the threshold at $\hbar\omega = 54.4$ eV. We see that the cross sections obtained in the two different ways are in very good agreement. This provides support for the proposition that the uncorrelated final states, Eq. (5), are indeed able to provide accurate information about photoelectrons emerging from helium asymptotically.

In [24] the strong dependence of the cross section as defined in Eq. (15) on the pulse length T as $\hbar\omega \rightarrow 54.4$ eV was discussed. It was demonstrated that σ , which seems to have a sharp rise, depends rather strongly on the pulse duration T in this limit. A possible explanation for this was considered: for finite T , there is also a finite spectral width of the pulse, enabling sequential double ionization also for central frequencies slightly below threshold. As the probability of se-

quential double ionization scales with T^2 , as opposed to T^1 in the nonsequential case, this gives rise to a pronounced increase in σ . The 4 fs pulse used in [24], although not long enough to resolve the cross section behavior very close to the threshold, was sufficient to observe the start of an increasing trend, and thus rejects the sequential overlap hypothesis with some confidence. However, in order to resolve the true behavior of the cross section in the immediate vicinity of the threshold, very narrow bandwidths, i.e., very long pulses, are required. By performing calculations with increasing pulse duration (up to 20 fs), we have confirmed that the value of σ does converge towards a well-defined value as T increases – also near the threshold. Moreover, as the spectral width of the pulse becomes so narrow that the overlap with the region in which sequential two-photon double ionization may take place vanishes, the pronounced rise in the cross section is seen to prevail. Hence, the fact that σ increases sharply as $\hbar\omega$ approaches 54.4 eV cannot be due to the final bandwidth of the pulse alone.

IV. CONCLUSION

We have investigated the role of electron correlations in obtaining the cross section for the process of nonsequential two-photon double ionization of helium, using two different methods of approach – by projection onto uncorrelated continuum states, and by imposing a complex absorbing potential within the proper many-body framework. The former has the advantage that these states are much easier to construct than the true two-electron continuum states, whereas no such states are needed in the latter method. Moreover, within this method single and double ionization yields may be obtained using a numerical grid considerably smaller than what is necessary to contain the ionized part of the two-particle wave function. The predictions of the methods were in agreement, thus suggesting that projecting the ionized part of the full wave function onto uncorrelated continuum states does provide correct ionization yields in the asymptotic limit.

Finally, we presented evidence that the cross section for this process remains well defined for photon energies arbitrarily close to the threshold at $\hbar\omega = 54.4$ eV (from below). The cross section is seen to have a sharp increase in this limit.

-
- [1] H. Mashiko, A. Suda, and K. Midorikawa, *Opt. Lett.* **29**, 1927 (2004).
 - [2] N. Miyamoto, M. Kamei, D. Yoshitomi, T. Kanai, T. Sekikawa, T. Nakajima, and S. Watanabe, *Phys. Rev. Lett.* **93**, 083903 (2004).
 - [3] Y. Nabekawa, H. Hasegawa, E. J. Takahashi, and K. Midorikawa, *Phys. Rev. Lett.* **94**, 043001 (2005).
 - [4] K. Hoshina, A. Hishikawa, K. Kato, T. Sako, K. Yamanouchi, E. J. Takahashi, Y. Nabekawa, and K. Midorikawa, *J. Phys. B* **39**, 813 (2006).
 - [5] W. Ackermann, *Nat. Photon.* **1**, 336 (2007).
 - [6] T. Shintake et al., *Nat. Photon.* **2**, 555 (2008).
 - [7] A. A. Sorokin, S. V. Bobashev, T. Feigl, K. Tiedtke, H. Wabnitz, and M. Richter, *Phys. Rev. Lett.* **99**, 213002 (2007).
 - [8] R. Moshhammer, Y. H. Jiang, L. Foucar, A. Rudenko, T. Ergler, C. D. Schröter, S. Lüdemann, K. Zrost, D. Fischer, J. Titze, et al., *Phys. Rev. Lett.* **98**, 203001 (2007).
 - [9] T. Laarmann et al., *Phys. Rev. A* **72**, 023409 (2005).
 - [10] H. Wabnitz et al., *Nature* **420**, 482 (2002).
 - [11] J. S. Parker et al., *Phys. Rev. Lett.* **96**, 133001 (2006).
 - [12] J. S. Parker, L. R. Moore, K. J. Meharg, D. Dundas, and K. T. Taylor, *J. Phys. B* **34**, L69 (2001).

- [13] L. R. Moore et al., J. Phys. Conf. Ser. **194**, 032055 (2009).
- [14] J. Colgan and M. S. Pindzola, Phys. Rev. Lett. **88**, 173002 (2002).
- [15] L. Feng and H. W. van der Hart, J. Phys. B **36**, L1 (2003).
- [16] S. Laulan and H. Bachau, Phys. Rev. A **68**, 013409 (2003).
- [17] B. Piraux, J. Bauer, S. Laulan, and H. Bachau, Eur. Phys. J. D **26**, 7 (2003).
- [18] S. X. Hu, J. Colgan, and L. A. Collins, J. Phys. B **38**, L35 (2005).
- [19] E. Fomouo, G. L. Kamta, G. Edah, and B. Piraux, Phys. Rev. A **74**, 063409 (2006).
- [20] R. Shakeshaft, Phys. Rev. A **76**, 063405 (2007).
- [21] I. A. Ivanov and A. S. Kheifets, Phys. Rev. A **75**, 033411 (2007).
- [22] D. A. Horner, F. Morales, T. N. Rescigno, F. Martín, and C. W. McCurdy, Phys. Rev. A **76**, 030701(R) (2007).
- [23] L. A. A. Nikolopoulos and P. Lambropoulos, J. Phys. B **40**, 1347 (2007).
- [24] J. Feist, S. Nagele, R. Pazourek, E. Persson, B. I. Schneider, L. A. Collins, and J. Burgdörfer, Phys. Rev. A **77**, 043420 (2008).
- [25] X. Guan, K. Bartschat, and B. I. Schneider, Phys. Rev. A **77**, 043421 (2008).
- [26] E. Fomouo, P. Antoine, B. Piraux, L. Malegat, H. Bachau, and R. Shakeshaft, J. Phys. B **41**, 051001 (2008).
- [27] A. Palacios, T. N. Rescigno, and C. W. McCurdy, Phys. Rev. A **79**, 033402 (2009).
- [28] R. Nepstad, T. Birkeland, and M. Førre, Phys. Rev. A **81**, 063402 (2010).
- [29] H. Hasegawa, E. J. Takahashi, Y. Nabekawa, K. L. Ishikawa, and K. Midorikawa, Phys. Rev. A **71**, 023407 (2005).
- [30] A. A. Sorokin, M. Wellhöfer, S. V. Bobashev, K. Tiedtke, and M. Richter, Phys. Rev. A **75**, 051402(R) (2007).
- [31] A. Rudenko, L. Foucar, M. Kurka, T. Ergler, K. U. Kühnel, Y. H. Jiang, A. Voitkiv, B. Najjari, A. Kheifets, S. Lüdemann, et al., Phys. Rev. Lett. **101**, 073003 (2008).
- [32] J. S. Briggs and V. Schmidt, J. Phys. B **33**, R1 (2000).
- [33] L. Avaldi and A. Huetz, J. Phys. B **38**, S861 (2005).
- [34] J. A. R. Samson, W. C. Stolte, Z.-X. He, J. N. Cutler, Y. Lu, and R. J. Bartlett, Phys. Rev. A **57**, 1906 (1998).
- [35] S. Selstø, and S. Kvaal, J. Phys. B **43**, 065004 (2010).
- [36] K. C. Kulander, Phys. Rev. A **35**, 445 (1987).
- [37] T. Fevens and H. Jiang, SIAM J. Sci. Comput. **21**, 255 (1999).
- [38] B. Feuerstein and U. Thumm, J. Phys. B **36**, 707 (2003).
- [39] M. Lein, E. K. U. Gross, and V. Engel, Phys. Rev. Lett. **85**, 4707 (2000).
- [40] D. Bauer and F. Ceccherini, Phys. Rev. A **60**, 2301 (1999).
- [41] D. G. Lappas and R. van Leeuwen, J. Phys. B **31**, L249 (1998).
- [42] S. L. Haan, P. S. Wheeler, R. Panfili, and J. H. Eberly, Phys. Rev. A **66**, 061402 (2002).
- [43] Z. Zhang, L.-Y. Peng, Q. Gong, and T. Morishita, Opt. Express **18**, 8976 (2010).
- [44] D. A. Horner, T. N. Rescigno, and C. W. McCurdy, Phys. Rev. A **77**, 030703(R) (2008).
- [45] P. Lambropoulos, L. A. A. Nikolopoulos, M. G. Makris, and A. Mihelic, Phys. Rev. A **78**, 055402 (2008).
- [46] D. A. Horner, T. N. Rescigno, and C. W. McCurdy, Phys. Rev. A **81**, 023410 (2010).
- [47] B. Piraux, E. Fomouo, P. Antoine, and H. Bachau, J. Phys. Conf. Ser. **141**, 012013 (2008).
- [48] T. Birkeland, R. Nepstad, and M. Førre, Phys. Rev. Lett. **104**, 163002 (2010).
- [49] W. S. Wilson and R. B. Lindsay, Phys. Rev. **47**, 681 (1935).
- [50] V. Gorini, A. Kossakowski, and E. Sudarshan, J. Math. Phys. **17**, 821 (1976).
- [51] G. Lindblad, Comm. Math. Phys. **48**, 119 (1976).
- [52] L. B. Madsen, L. A. A. Nikolopoulos, and P. Lambropoulos, Eur. Phys. J. D **10**, 67 (2000).
- [53] E. S. Smyth, J. S. Parker, and K. Taylor, Comput. Phys. Commun. **114**, 1 (1998).
- [54] H. A. Leth, L. B. Madsen, and K. Mølmer, Phys. Rev. Lett. **103**, 183601 (2009).
- [55] M. Feit, J. Fleck, and A. Steiger, J. Comput. Phys. **47**, 412 (1982).
- [56] T. Birkeland and R. Nepstad, *Pyprop*, <http://pyprop.googlecode.com>.
- [57] D. E. Manolopoulos, J. Chem. Phys. **117**, 9552 (2002).